

Coulomb effects in the ${}^3\text{He}$ ground state

J. L. Friar and B. F. Gibson

Theoretical Division, Los Alamos National Laboratory, Los Alamos, New Mexico 87545

G. L. Payne

Department of Physics and Astronomy, University of Iowa, Iowa City, Iowa 52242

(Received 1 December 1986)

The effect of the proton-proton Coulomb interaction in the ${}^3\text{He}$ ground state is investigated. The rms radii, first-order and second-order Coulomb energy shifts, the validity of the hyperspherical approximation, and the various trinucleon densities are examined.

I. INTRODUCTION

Most investigations of the trinucleon bound states have assumed charge symmetry and charge independence. That is, one assumes a common interaction between two protons, two neutrons, and the (isospin) $T=1$ part of the neutron-proton interaction. Isospin is conserved and the trinucleons form a (pure) isodoublet state. Many diverse mechanisms break isospin symmetry. Primary among them in the trinucleons is the Coulomb interaction between the two protons in ${}^3\text{He}$.¹⁻⁵

The mass difference between the mirror pairs ${}^3\text{He}$ and ${}^3\text{H}$ is a direct manifestation of charge-symmetry breaking. A major element of this is the mass difference of a free neutron and a free proton: 1.293 MeV. Subtracting these leads to a ${}^3\text{H}$ - ${}^3\text{He}$ binding energy difference of 764 keV. It has been known for 50 years⁶ that the bulk of this difference is due to the pp Coulomb interaction in ${}^3\text{He}$, although only recently has a quantitative understanding been achieved.⁷⁻¹⁰ One of our goals in this work is to extend this understanding.

Two-body potential models tend to underbind the triton.¹¹ There is a strong correlation between the size and the amount of binding: As binding decreases, the system swells, and the Coulomb energy will decrease. In order to treat the Coulomb energy in the absence of a detailed understanding of the underlying strong interaction dynamics, the hyperspherical approximation was developed.^{7,8} In first-order perturbation theory in the fine structure constant, α , and assuming the impulse approximation for the nuclear charge density, one finds

$$\begin{aligned} E_C^H &= \frac{\alpha}{\sqrt{3}} \int d^3r [\rho_s(r) + \rho_d(r)] \frac{g(r)}{r} \\ &= \frac{\alpha}{3\sqrt{3}} \int d^3r [4\rho_{{}^3\text{He}}(r) - \rho_{{}^3\text{H}}(r)] \frac{g(r)}{r}, \end{aligned} \quad (1)$$

where $g(r)$ determines the effect of the nucleon charge distribution on the Coulomb potential¹ and $\rho_s(r)$ and $\rho_d(r)$ are the isoscalar and "difference" charge densities¹² of ${}^3\text{He}$ and ${}^3\text{H}$:

$$Z\rho_{\text{ch}}(r) = Z\rho_s(r) \pm \rho_d(r), \quad (2)$$

where the upper sign corresponds to ${}^3\text{He}$ ($Z=2$) and the

lower to ${}^3\text{H}$ ($Z=1$). All charge densities are normalized according to $\int \rho(r) d^3r = 1$, except for ρ_d , which is normalized to zero. The significant feature of this approximation is that the Coulomb energy, whose evaluation involves an integration over the appropriate two-body correlation function, can be approximated by a quadrature involving the charge density, a one-body operator. Moreover, the latter is known experimentally. Note that the isospin structure weights the ${}^3\text{He}$ data by a factor of 4. That numerical result^{9,10} is $E_C^H \cong 638 \pm 10$ keV.

In addition to the first-order Coulomb energy, a very small second-order contribution¹ arises. This quantity also depends sensitively on the binding energy. We will elucidate its properties and demonstrate its smallness.

A much more interesting quantity is the rms charge radius of ${}^3\text{He}$. If we assume⁵ that the asymptotic wave function dominates the matrix element of r^2 , then the rms radius should be proportional to $E_B^{-1/2}$. This was previously shown to be the case for the isoscalar (mass) radius. The repulsive Coulomb interaction will decrease E_B by roughly 10% and, concomitantly, increase the radius by roughly 5%. However, the repulsive Coulomb (Gamow) barrier will also modify (lower) the tail of the wave function, and this will tend to decrease the ${}^3\text{He}$ radius. The size of the latter effect is not known and will be investigated. Recent tritium data from Saclay¹³ and new data from MIT¹⁴ have rekindled interest in the radii.

In the course of investigating convergence properties of solutions of the Faddeev equation with diverse combinations of two- and three-body potentials and numbers of channels (i.e., partial waves), many wave functions corresponding to a wide range of eigenvalues were obtained.¹¹ These wave functions can be used to calculate observables, and form a kind of "theoretical" data base. We previously found that many of these observables, when plotted versus the corresponding binding energy, exhibited scaling with that energy. That is, they exhibit a simple functional behavior, with only a small spread of values for fixed E_B . Fits to these plots, extrapolated to the correct binding energy, probably provide the best theoretical estimates of these trinucleon observables, providing that scaling obtains. Previously this technique was applied to the triton, and will be employed here for ${}^3\text{He}$ with a pp Coulomb interaction included. Some caution is indicated, however.

If the data set is limited to models which do not include the correct physics, a false result could be obtained.

The Faddeev equations are exactly equivalent to the Schrödinger equation. There are, however, alternative ways^{2,3,15} to include the Coulomb interaction (or three-body forces) with the short-range two-body forces in the former equations. Although they are all equivalent in principle, they differ in practice when the Faddeev equations are partial-wave truncated (i.e., a limited number of channels is employed). Because the Coulomb force is long-ranged, partial-wave truncation can lead to a deficient force. We employ a nonstandard version of the Faddeev equations which correctly describes the Coulomb distortion when a proton is far away from the remaining charged particle. Thus our Faddeev eigenvalues are closer to the non-Coulomb eigenvalues, augmented by the Coulomb energy calculated in perturbation theory, than those calculated with the standard partial-wave truncated Faddeev equations which include a Coulomb force. We will ignore the coupling to the isoquartet channel (a very good approximation¹) and employ a point Coulomb interaction for specificity in calculating our wave functions. We have also implemented a technical improvement¹⁶ in calculating our matrix elements.

II. RESULTS

The ${}^3\text{He}$ charge radii obtained from our wave function sets, one with the Coulomb interaction and the other without, are displayed in Fig. 1, together with simple fits.

The Coulomb energy shift is evident in the dashed curve, and the Coulomb barrier separates the two curves by approximately 0.04 fm for $E_B = 7.75$ MeV. Figure 2 displays the same Coulomb distorted ${}^3\text{He}$ result, together with the (non-Coulomb) ${}^3\text{H}$ results and data from a recent Saclay analysis.¹³ The data are in good agreement with the fits at the appropriate (experimental) binding energies (1.58 fm for ${}^3\text{H}$ and 1.77 fm for ${}^3\text{He}$), although the ${}^3\text{He}$ results would not be in agreement with the non-Coulomb fit at the physical ${}^3\text{He}$ binding energy, which is shifted (upward) by approximately 0.08 fm from the triton result. The net result of these competing Coulomb effects is an increase of 0.04 fm in the ${}^3\text{He}$ radius.

The Coulomb energy is given quite accurately by first-order perturbation theory.

$$E_C^{(1)} = \langle \Psi_0 | V_C | \Psi_0 \rangle, \quad (3)$$

where V_C is the Coulomb interaction incorporating (for specificity) a dipole proton form factor¹ and Ψ_0 is the ${}^3\text{H}$ wave function. These results are shown in Fig. 3. At the physical triton binding energy the fit produces $E_C^{(1)} \cong 652 \pm 2$ keV.

One can also calculate the expectation value of V_C with respect to Coulombic wave functions $\Psi \cong \Psi_0 + \Delta\Psi$:

$$\begin{aligned} \bar{E}_C &= \langle \Psi | V_C | \Psi \rangle \cong \langle \Psi_0 | V_C | \Psi_0 \rangle + 2\langle \Psi_0 | V_C | \Delta\Psi \rangle \\ &= E_C^{(1)} + 2E_C^{(2)}, \end{aligned} \quad (4)$$

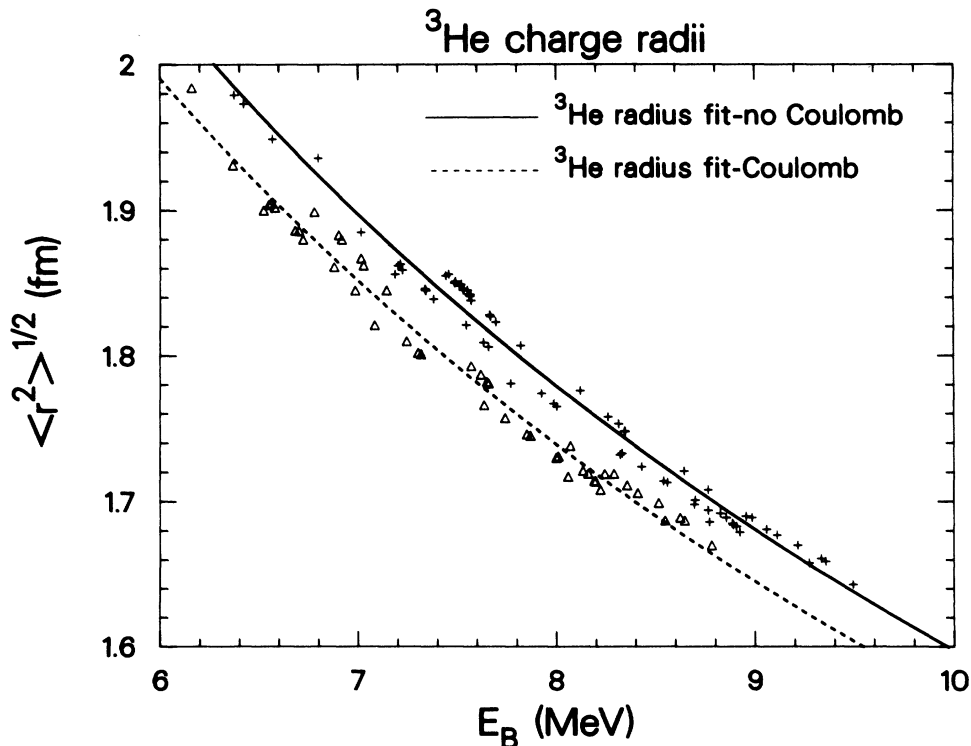


FIG. 1. rms charge radii of ${}^3\text{He}$ for diverse two-body and three-body force models, with and without a pp Coulomb interaction, plotted versus binding energy.

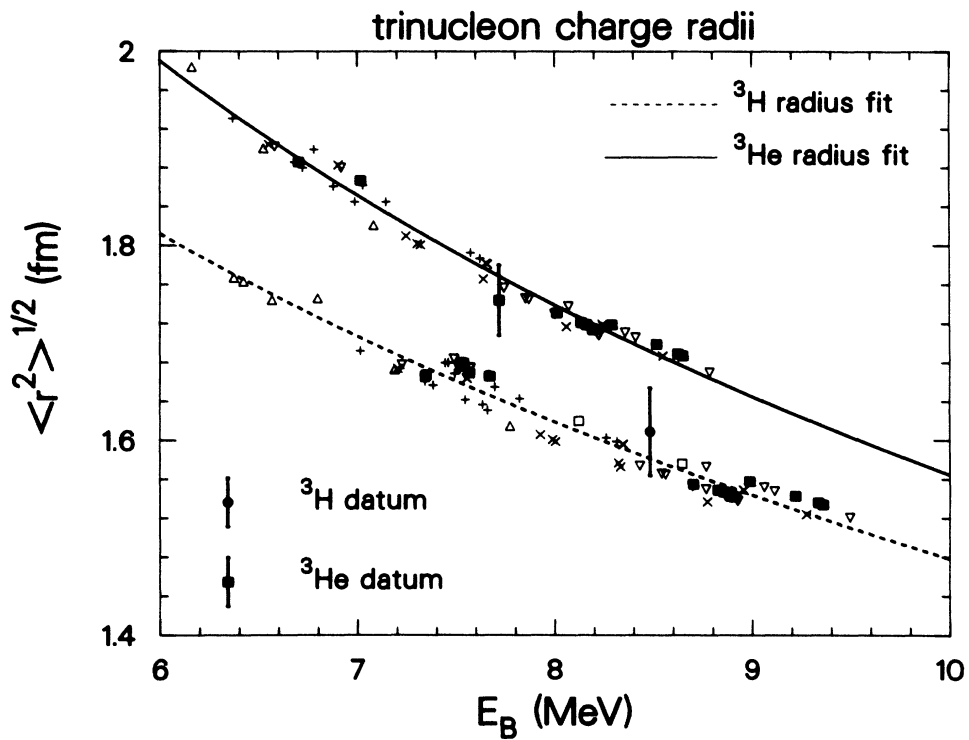


FIG. 2. Trinucleon rms charge radii plotted versus the corresponding binding energy for diverse two-body and three-body force models.

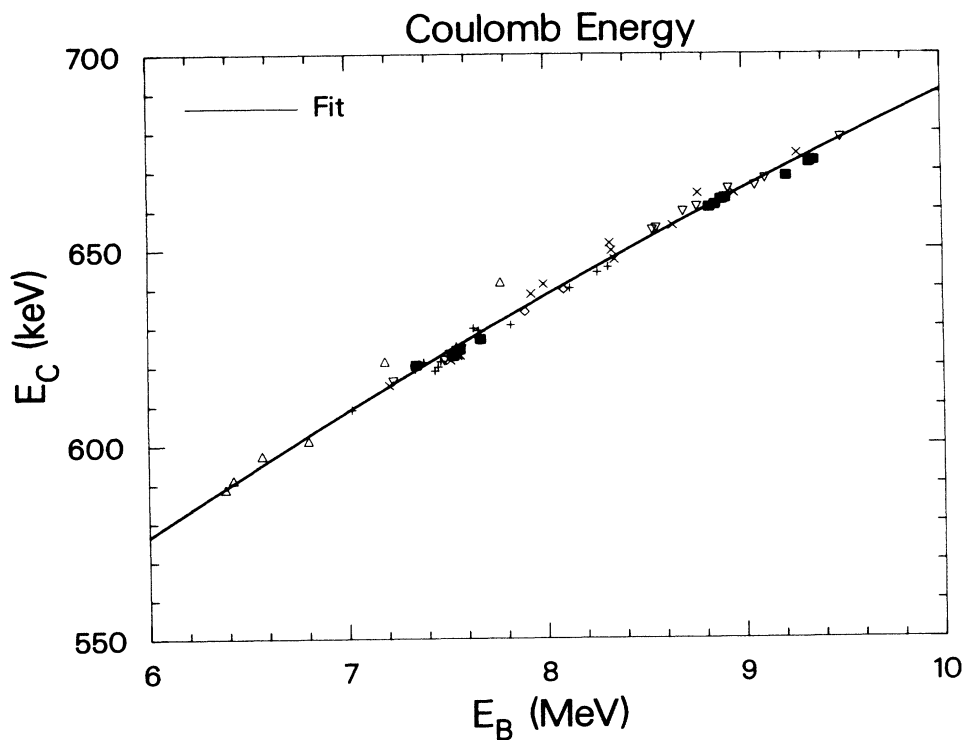


FIG. 3. ${}^3\text{He}$ Coulomb energy in first-order perturbation theory for the models in Fig. 1, plotted versus binding energy.

where we have assumed that we can neglect third-order contributions (in α) to

$$E_C = E_C^{(1)} + E_C^{(2)} + \dots, \quad (5)$$

and therefore second-order (in α) corrections to Ψ . Equations (4) and (5) can be solved¹ to yield

$$E_C^{(2)} \cong [\bar{E}_C - E_C^{(1)}]/2. \quad (6)$$

Comparison of corresponding members of the two wave function sets produces the results of Fig. 4 for

$$E_C^{(2)} = - \sum_{N \neq 0} \frac{\langle \Psi_0 | V_C | N \rangle \langle N | V_C^0 | \Psi_0 \rangle}{E_N - E_0}. \quad (7)$$

The wave functions were calculated using the point Coulomb interaction, V_C^0 while the operator V_C can be taken to be the point Coulomb interaction or one modified by a nucleon charge distribution. This leads to the two separate results for $E_B = 8.5$ MeV: -4.4 and -3.9 keV. The curves are separated by approximately 0.5 keV. Had we also produced a result for both Coulomb interactions in Eq. (7) modified by the nucleon finite size, it would lie about 0.5 keV lower still (or -3.4 keV), as indicated by the sparse calculations of Ref. 1. In that reference we argued that the $E_C^{(2)}$ should scale roughly as $[E_C^{(1)}]^2/E_B$. The dependence on the triton binding energy, E_B , is actually somewhat stronger than this ($\sim E_B^{-0.9}$).

The results for the hyperspherical approximation to the Coulomb energy have been presented before.⁵ Because the

hyperspherical approximation to the two-body correlation function lacks the hole present at short distances in the true correlation function, the values of E_C^H are larger than $E_C^{(1)}$ by slightly more than 1%. On the other hand, the use of the ${}^3\text{He}$ Coulomb modified charge form factor or charge density in Eq. (1) ($\langle \Psi | \rho | \Psi \rangle$) leads to an overestimate¹ of the second-order Coulomb energy by roughly $\frac{5}{3}E_C^{(2)}$. The numerical factor arises from $\frac{4}{3}$ of the ${}^3\text{He}$ density times 2 (there are two Coulomb modified wave functions in the ${}^3\text{He}$ charge density) minus the normal amount (1) of $E_C^{(2)}$. This leads to roughly -6 keV which must be subtracted out, or an increase of 6 keV in the hyperspherical estimate of the Coulomb energy. The latter number offsets the inherent overestimate of $E_C^{(1)}$ by the hyperspherical method, which is also roughly 1%.

We note also that the percentages of P - and D -wave components are virtually unchanged by the Coulomb interaction, while the S -state probability drops substantially, reflecting the strong binding energy dependence of that quantity found earlier⁵ ($\sim E_B^{-2}$).

Finally, we present in Fig. 5 the results for various densities calculated in impulse approximation. The results labeled " ${}^3\text{He}$ " were calculated using 34 channels and the Reid Soft Core (RSC) two-body potential including a Tucson-Melbourne three-body force (TBF) together with a pp Coulomb force. The " ${}^3\text{H}$ " case is analogous, but the Coulomb force is omitted. The large difference between neutron densities (or proton densities) is due to the difference between np and nn or pp forces. The proton (or

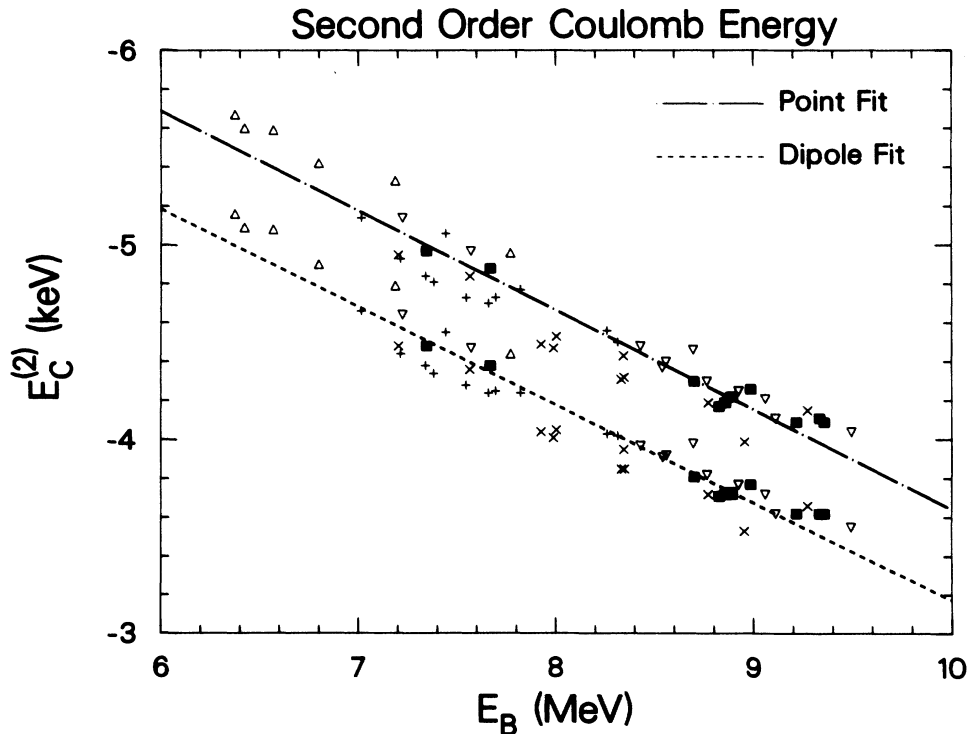


FIG. 4. Second-order ${}^3\text{He}$ Coulomb energy for the models in Fig. 1, plotted versus binding energy. The upper and lower curves correspond to different Coulomb force models as described in the text.

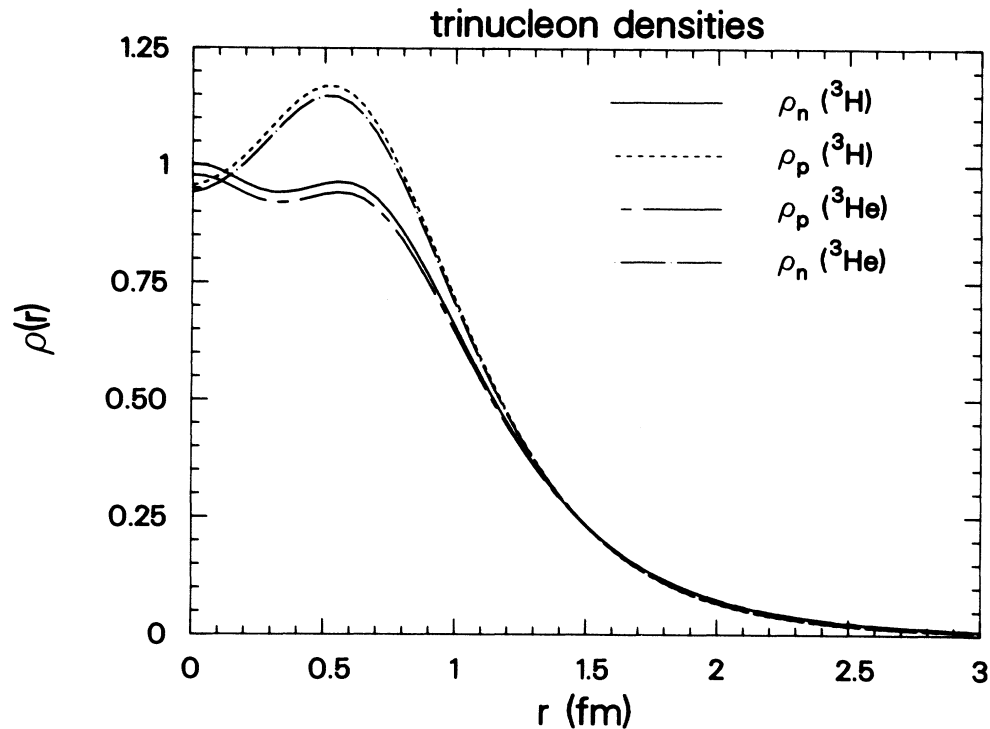


FIG. 5. Trinucleon proton and neutron densities in impulse approximation calculated with (${}^3\text{He}$) and without (${}^3\text{H}$) a pp Coulomb interaction. These densities are 4π times the ones defined in Eqs. (1) and (2).

charge) densities were previously presented¹² without a Coulomb interaction. In impulse approximation, neglecting charge-symmetry breaking, the neutron density of ${}^3\text{H}$ and the proton density of ${}^3\text{He}$ are identical; similarly, the neutron density of ${}^3\text{He}$ would be identical to the proton density of ${}^3\text{H}$. The small difference between $\rho_n({}^3\text{H})$ and $\rho_p({}^3\text{He})$ is virtually the same as that found several years ago⁴ for the five-channel case without a TBF. The tails of these densities are all rather different. A diminution of the density inside the nucleus reflects an enhancement in the tail, for reasons described earlier. The crossover point is roughly 1.5 fm. At 3.0 fm the Coulomb modified densities are roughly 6% larger than the corresponding unmodified ones.

Knowing the neutron and proton mass densities (and the nucleon-nucleon correlation functions) of ${}^3\text{H}$ and ${}^3\text{He}$ is of fundamental importance to the interpretation of scattering data involving strong probes. For example, the differences seen in π^\pm scattering from the trinucleons has been cited as evidence for a charge symmetry violation.¹⁷

The unanswered question is whether the observed differences in the cross section ratios can be explained in terms of known charge-symmetry violating effects such as the Coulomb interaction.

III. CONCLUSIONS

The rms radius of ${}^3\text{He}$ is modified by the Coulomb interaction in two ways. The diminution of binding increases the size (roughly) according to $E_B^{-1/2}$, while the smaller modification from the Coulomb barrier reduces the size. The net effect is a small increase in the radius. The first-order perturbation theory result for the Coulomb energy of ${}^3\text{He}$ is rather sensitive to binding, as is the second-order contribution. The latter, however, is very small (~ -4 keV). The hyperspherical approximation to the Coulomb energy works well (at the 99% level). There is a non-negligible (but small) Coulomb effect on the various trinucleon densities.

¹G. L. Payne, J. L. Friar, B. F. Gibson, Phys. Rev. C 22, 832 (1980) contains references to the previous work and a discussion of many technical details.

²J. L. Friar, B. F. Gibson, D. R. Lehman, and G. L. Payne, Phys. Rev. C 25, 1616 (1982).

³J. L. Friar, B. F. Gibson, and G. L. Payne, Phys. Rev. C 28, 983 (1983). References 2 and 3 discuss alternative formulations of the Faddeev equations with a Coulomb interaction.

⁴J. L. Friar, B. F. Gibson, E. L. Tomusiak, and G. L. Payne, Phys. Rev. C 24, 665 (1981).

- ⁵J. L. Friar, B. F. Gibson, C. R. Chen, and G. L. Payne, Phys. Lett. **161B**, 241 (1985).
- ⁶H. Bethe and R. F. Bacher, Rev. Mod. Phys. **8**, 82 (1936).
- ⁷M. Fabre de la Ripelle, Fizika (Zagreb) **4**, 1 (1972).
- ⁸J. L. Friar, Nucl. Phys. **A156**, 43 (1970).
- ⁹R. A. Brandenburg, S. A. Coon, and P. U. Sauer, Nucl. Phys. **A294**, 305 (1978).
- ¹⁰J. L. Friar and B. F. Gibson, Phys. Rev. C **18**, 908 (1978).
- ¹¹C. R. Chen, G. L. Payne, J. L. Friar, and B. F. Gibson, Phys. Rev. C **31**, 2266 (1985); **33**, 1740 (1986).
- ¹²J. L. Friar, B. F. Gibson, G. L. Payne, and C. R. Chen, Phys. Rev. C **34**, 1463 (1986).
- ¹³F.-P. Juster *et al.*, Phys. Rev. Lett. **55**, 2261 (1985); S. Platchkov and B. Frois, private communication.
- ¹⁴D. Beck, private communication.
- ¹⁵T. Sasakawa and T. Sawada, Phys. Rev. C **20**, 1954 (1979).
- ¹⁶J. L. Friar, E. L. Tomusiak, B. F. Gibson, and G. L. Payne, Phys. Rev. C **24**, 677 (1981).
- ¹⁷B. M. K. Nefkens *et al.*, Phys. Rev. Lett. **52**, 735 (1984).